JOURNAL OF CATALYSIS 127, 605–618 (1991)

Hydrodenitrogenation of Decahydroquinoline, Cyclohexylamine and *O*-Propylaniline over Carbon-Supported Transition Metal Sulfide Catalysts

S. EIJSBOUTS,[1] C. SUDHAKAR,[2] V. H. J. DE BEER, AND R. PRINS[3]

Laboratory for Catalysis, Eindhoven University of Technology, P.O. Box 513, 5600 MB Eindhoven, The Netherlands

Received April 11, 1990; revised August 3, 1990

Carbon-supported transition metal sulfide (TMS) catalysts were prepared by impregnation of an activated carbon support with aqueous solutions of first-, second-, and third-row (group V–VIII) transition metal salts followed by drying and *in situ* sulfidation. Their activity for the hydrodenitrogenation of decahydroquinoline (5.2–5.5 MPa, 623–653 K), cyclohexylamine (4.8–5.5 MPa, 543–653 K), and *o*-propylaniline (5.1–5.5 MPa, 593–653 K) was tested in microautoclaves. When plotted versus the position of the transition metal in the Periodic System, the conversions of all three N-containing reactants to hydrocarbons over the first-row transition metal sulfides formed U-shaped curves with a minimum at Mn, while V had the highest conversion. The decahydroquinoline and cyclohexylamine conversions to hydrocarbons over the second- and third-row TMS formed volcano curves with maxima at Rh and Ir, respectively. Disproportionation reactions were found to be important side reactions in the cyclohexylamine hydrodenitrogenation. The activities of the second-row transition metal sulfides for the conversion of *o*-propylaniline formed a volcano curve with a maximum at Ru or Rh sulfide, whereas the activities of the third-row transition metal sulfides formed a strongly distorted volcano curve. All catalysts and especially Re sulfide had a very high selectivity for propylbenzene.

INTRODUCTION

The hydrotreatment of heavy crudes and the further treatment of vacuum residues of oil distillation have increased considerably in the past decade. Heavy crudes and vacuum residues contain relatively high percentages of S, N, O, and metals (Ni, V) and make high demands on the catalyst performance. If not removed, N-compounds act as poison for hydrocracking and reforming catalysts in the later stages of oil refining. The presence of N-compounds leads to poor color, smell, and stability of the final products and subsequently causes NO_x pollution of the atmosphere. Furthermore, the intensified protection of the environment has led to the sharpening of the norms for the S, N, and metal content of the petroleum products. The hydrodenitrogenation (HDN) reaction as one of the most demanding hydrotreatment steps has therefore become very important.

The HDN reaction consists of a sequence of reactions: a hydrogenation of the N-containing aromatic ring, a ring-opening reaction, and the N-removal via hydrogenolysis or elimination. Since the C–N bond in heterocyclic aromatic compounds is much stronger than the comparable C–S or C–O bond, the N-containing ring (and to a large extent also the neighboring benzene ring) must be hydrogenated before the ring opening reaction can take place. Unfortunately, the saturated N-containing compounds are excellent coke-precursors and can lead to permanent poisoning of catalysts which do

[1] Present address: AKZO Chemicals B.V. Research Centre, P.O. Box 15, 1000 AA Amsterdam, The Netherlands

[2] Present address: Texaco Research Center, P.O. Box 509, Beacon, NY 12508, USA

[3] Present address: Technisch Chemisches Laboratorium, ETH, 8092 Zürich, Switzerland

0021-9517/91 $3.00

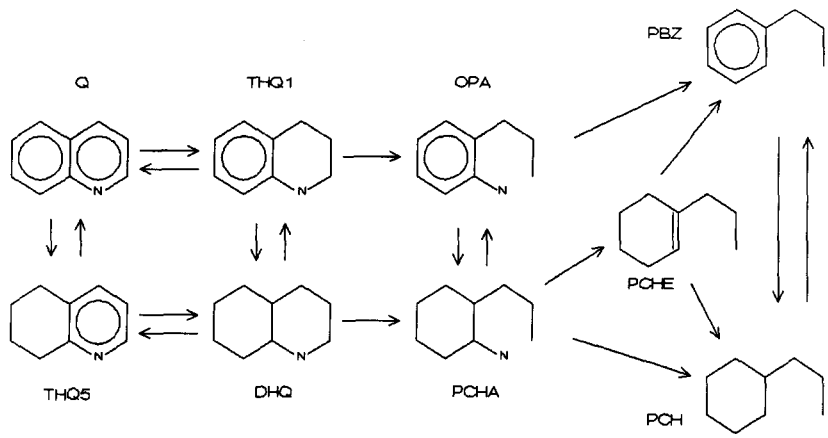

FIG. 1. Reaction network of the HDN of quinoline. Q, quinoline; THQ1, 1,2,3,4-tetrahydroquinoline; THQ5, 5,6,7,8-tetrahydroquinoline; DHQ, decahydroquinoline; OPA, *o*-propylaniline; PCHA, propylcyclohexylamine; PCHE, propylcyclohexene; PBZ, propylbenzene; PCH, propylcyclohexane.

not have sufficient activity for the N-removal. Besides, a high hydrogenation activity is very important in the hydrotreatment of heavy feed. In this type of hydrotreatment, not only S, N, O, and metals must be removed, but also the average molecular weight as well as the C/H ratio must be reduced, making hydrocracking and hydrogenation important reactions.

The design of hydrotreating catalysts with good HDN activity and selectivity requires sufficient knowledge of the influence of the active phase, support, and additives on the performance of the catalyst. The catalytic properties of various transition metals in reactions such as hydrogenation, hydrogenolysis, isomerization, and hydrocarbon oxidation have been studied extensively (*1–3*). When their activities are plotted versus the position in the Periodic Table, so-called volcano-type curves are obtained, which reflect the periodicity of physical and chemical properties of the transition metals. Recently, similar studies were made of the behavior of transition metal sulfides (TMS) as catalysts in hydrodesulfurization (HDS) reactions. For the high-pressure dibenzothiophene HDS over bulk TMS (first-, second-, and third-row, groups VI–VIII), Pecoraro and Chianelli (*4*) found a double maximum curve (Cr, Co) for the first row and volcano curves for the second- and third-row TMS with maxima at Ru and Os, respectively. Similar trends have been found in the low-pressure thiophene HDS by Vissers *et al.* (*5*) and by Ledoux *et al.* (*6*) for carbon-supported first-, second-, and third-row TMS from groups VI–VIII and I–VIII, respectively. The carbon-supported Rh and Ir sulfides gave the highest activity among the second- and third-row TMS. Attempts have been made to find correlations between the HDS activity and the heats of formation (*7–10*), the electronic structures (*7–10*), and the crystal structures (*6*) of the TMS.

Recently we investigated the activities and selectivities of first-, second-, and third-row (groups V–VIII) transition metal sulfides supported on carbon in the HDN of quinoline (*11, 12*). Ledoux and Djellouli investigated the HDN of pyridine over carbon-supported second-row transition metal sulfides (*13*). The HDN network of quinoline has been studied in detail by Satterfield and co-workers (*14–18*), Schulz *et al.* (*19*), and Gioia and Lee (*20*) and has proved of great use for an understanding of HDN in general. It is presented in Fig. 1. The main

reaction pathway starts with hydrogenation of quinoline (Q) via 1,2,3,4-tetrahydroquinoline (THQ1) or 5,6,7,8-tetrahydroquinoline (THQ5) to decahydroquinoline (DHQ). DHQ then undergoes ring opening via elimination or hydrogenolysis to propylcyclohexylamine (PCHA), which rapidly converts to hydrocarbons via hydrogenolysis to propylcyclohexane (PCH), or via NH_3 elimination to propylcyclohexene (PCHE), which can react further to PCH and propylbenzene (PBZ). In both cases PCH is the main reaction product. A second reaction pathway includes the ring-opening reaction of THQ1 to orthopropylaniline (OPA). OPA can be hydrogenolyzed directly to PBZ, or first hydrogenated to PCHA and subsequently converted to hydrocarbons as in the main reaction pathway (cf. Fig. 1).

It is obvious that the Q–HDN reaction network includes all the important steps (hydrogenation, ring-opening, and N-removal) of hydrodenitrogenation. The Q–HDN reaction network is very complex, however, and it is difficult to separate the different reaction steps by a study of the HDN of quinoline alone. Therefore we have also studied the HDN of decahydroquinoline, as the key intermediate in the main route of Q–HDN, and the HDN of OPA, the key intermediate in the second Q–HDN route. We present the results of our investigation in two papers. In the present paper we present the results of the HDN of decahydroquinoline (DHQ), cyclohexylamine (CHA), and orthopropylaniline (OPA). In the second paper (*21*) we discuss the results of the HDN of quinoline itself. By first presenting the HDN of intermediate products of the HDN of quinoline we are able to explain in the second paper the different roles of kinetics and adsorption, and the role of intermediates.

TABLE 1

HDN of Decahydroquinoline
(5.0–5.5 MPa, 623 and 653 K)

Catalyst[a]	Product composition[b]						
	N_{hc}	n_{pch}	n_{pbz}	n_{pche}	N_{dhq}	N_{thq5}	N_{thq1}
T(sulf.) = *T*(react.) = 653 K, *t*(react.) = 3 h							
C	26	53	16	30	38	32	2
V(4.8)/C	47	59	15	26	13	32	6
Cr(4.9)/C	31	44	21	35	34	32	2
Mn(5.2)/C	21	51	17	32	49	28	2
Fe(5.3)/C	23	54	17	29	44	29	2
Co(5.6)/C	23	43	20	36	29	42	5
Ni(5.6)/C	29	48	19	34	20	20	9
T(sulf.) = *T*(react.) = 653 K, *t*(react.) = 1.5 h							
Mo(8.8)/C	23	43	15	42	24	41	7
Ru(9.2)/C	36	88	3	9	22	25	12
Rh(9.3)/C	57	89	5	7	10	16	7
Pd(9.6)/C	52	94	5	1	20	17	8
W(15.5)/C	19	41	17	42	30	40	6
Re(15.7)/C	22	70	11	19	26	31	14
Os(16.0)/C	42	81	12	8	24	21	8
Ir(16.1)/C	84	96	2	2	6	3	1
Pt(16.3)/C	20	77	5	18	30	41	8
T(sulf.) = *T*(react.) = 623 K, *t*(react.) = 3 h							
blank[c]	3	42	22	36	94	3	1
C	2	53	9	39	93	5	0
Mo/C	37	46	18	36	47	13	3
Ru/C	41	68	12	21	40	11	7
Rh/C	48	94	3	3	38	9	4
Pd/C	22	71	10	19	60	16	2
W/C	13	45	20	34	69	17	2
Re/C	33	67	12	22	47	12	6
Os/C	57	82	6	12	29	7	5
Ir/C	95	99	1	1	4	1	0
Pt/C	36	82	4	13	46	14	5

[a] Numbers within parentheses are the wt% of metals.
[b] N_x are mol% DHQ converted to compound x, and $n_x = N_x/N_{hc}$ is the selectivity (in percentage) for compound x.
[c] Empty reactor.

EXPERIMENTAL

The activated carbon support (Norit RX3 extra: surface area, 1190 m^2g^{-1}; pore volume, 1.0 cm^3g^{-1}) was impregnated with aqueous solutions of group V–VIII transition metal salts (mostly chlorides (*5*)) and dried in air at 383 K (in 3 h from 293 to 383 K, 16 h at 383 K). The surface loading of all catalysts was approximately 0.5 metal atoms nm^{-2}, and the respective wt% are listed in Table 1. The notation used in the text is Me/C.

The reaction was carried out in stirred microautoclaves (*22*) (volume, 20 cm^3) according to the following procedure. A 12.5 mg sample of the dried catalyst was sulfided *in situ* using a mixture of 10% H_2S in H_2 (Air Products, $H_2 > 99.99\%$, $H_2S > 99.9\%$) (60 std cm^3 min^{-1}, 6 K min^{-1} from 293 to the desired temperature in the range 593–653 K, and held 1 h at that temperature, 0.1 MPa). After sulfidation the catalyst was cooled to room temperature in the H_2S/H_2 atmosphere. The liquid storage vessel filled with 2 cm^3 of the reactant mixture, containing either 3.9 mol% DHQ (Alfa Products, *cis* and *trans*) and 0.5 mol% $(CH_3)_2S_2$ in hexadecane (both Janssen Chimica, >99%), 4.7 mol% CHA, and 0.5 mol% $(CH_3)_2S_2$ in hexadecane (all three Janssen Chimica, >99%), or 4.0 mol% OPA (Janssen Chimica, >97%) and 0.5 mol% $(CH_3)_2S_2$ in hexadecane (both Janssen Chimica, >99%), was pressurized with H_2 (Hoekloos, $H_2 > 99.99\%$) and the liquid was injected into the autoclave. During this stage of the experimental procedure a small amount of air can enter the autoclave. However, the amount of $(CH_3)_2S_2$ in the reaction mixture ensures that the catalyst remains sulfided during the reaction. The pressure in the autoclave was adjusted to 4.0 MPa, the stirring was started and the temperature was increased (6 K min^{-1}) to 623 or 653 K (DHQ–HDN), to 543, 553, or 593 K (CHA–HDN), and to 593, 613, or 653 K (OPA–HDN) (see Tables 1–3) and held for 3 or 1.5 h (reaction pressure approximately 4.8 MPa at 543 K, 5.1 MPa at 593 K, and 5.5 MPa at 653 K). After the reaction the autoclave was cooled rapidly (20 min) and the liquid was removed and analyzed by a gas chromatograph using a 50-m-capillary CPSil-5 column (Chrompack) with temperature programming and an FID detector.

RESULTS AND DISCUSSION

Decahydroquinoline HDN

The results of the DHQ–HDN experiments are listed in Table 1. In this and the other Tables, N_x stands for the mol% of feed converted to compound x, and n_x is the selectivity for compound x in percentage ($n_x = N_x/N_{hc}$ for hydrocarbons and $n_x = N_x/N_n$ for the double-ring N-compounds). Besides unreacted DHQ and the final hydrocarbon products, the reaction mixture contained considerable amounts of THQ5 and THQ1 and small amounts of Q (in all cases less than 3 mol%, except for the empty reactor which produced 15% Q) and OPA ($N_{opa} = 9$ for Rh/C, 5 for Ir/C, and less than 4 mol% for all other catalysts). The reaction mixture contained only a small amount of cracking and isomerization products (less than 3 mol%), which was not taken into account in the evaluation of the results, i.e., $N_{hc} + N_n + N_{opa} = 100$. The DHQ–HDN activity and the product distribution of a number of TMS catalysts (e.g., Ru/C, Os/C, Mo/C, Pd/C) were dependent on the sulfidation and reaction temperature (Table 1). The presence of THQ5, THQ1, Q, and OPA indicates that the "back" reactions of DHQ to THQ5 and THQ1, and further to Q and OPA, cannot be neglected relative to the "forward" reaction of DHQ to hydrocarbons. Especially the THQ5 concentrations were appreciable. If we assume that the hydrogen concentration stays constant during reaction, a qualitative analysis of our results can in some cases already give information on the relative magnitudes of the rate constants k_{-1} and k_2 for the DHQ → THQ5 and DHQ → hydrocarbons reactions, respectively. Namely, when first-order Langmuir–Hinshelwood kinetics are applicable, then the concentration of THQ5 can only be larger than that of the hydrocarbons when $k_{-1} > k_2$.

$$\text{THQ5} \underset{k_1}{\overset{k_{-1}}{\rightleftarrows}} \text{DHQ} \xrightarrow{k_2} \text{hydrocarbons}$$

For all first-row TMS/C, and Mo/C, W/C, Re/C, and Pt/C at 653 K, thus, it can be directly concluded that k_{-1} is larger than k_2. In the other cases we cannot draw definitive conclusions from out data, but we can safely say that in all cases the rate constant for dehydrogenation of DHQ to THQ5 was not much smaller than the rate constant for con-

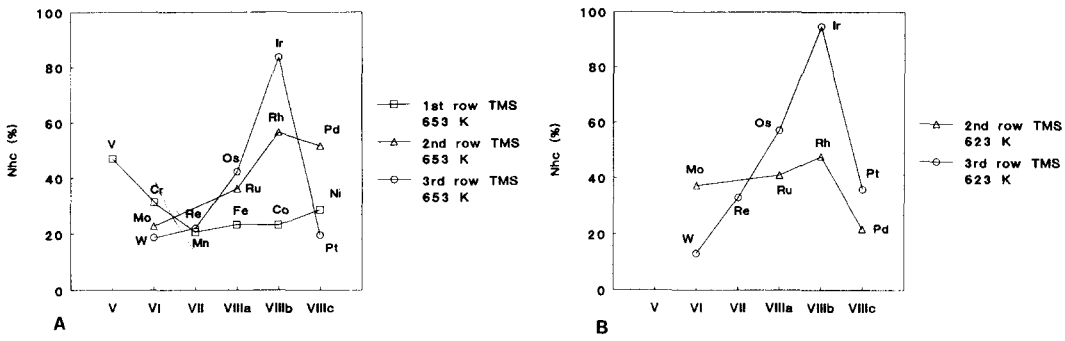

FIG. 2. Conversion of decahydroquinoline to hydrocarbons (N_{hc}, %) over carbon-supported transition metal sulfide catalysts at 653 K (A) and 623 K (B) as a function of the position of the transition metals in the Periodic Table.

version of DHQ to hydrocarbons. The observed differences between the catalysts at different temperatures are most certainly due to the changes of the reaction mechanism with temperature (shift of the hydrogenation equilibrium to the unsaturated N-compound, the equilibrium DHQ/THQ5 ratio being 1.5 at 623 K and 0.3 at 653 K (*14*), and an increase of the rate of the elimination reaction with increasing temperature), and possibly also partly due to a different degree of sulfidation of the catalysts.

The fact, in contradiction to thermodynamic predictions (*14*), that amounts of THQ5 larger than those of THQ1 and Q were observed is due to the weak kinetic coupling of the THQ5 ⇆ DHQ part of the Q, THQ1, THQ5, DHQ kinetic network with the Q ⇆ THQ1 part (cf. Fig. 1). As argued above, the rate constant for the reaction of DHQ to THQ5 is in most cases of the same order of magnitude as that of the reaction of DHQ to hydrocarbons. Therefore, appreciable amounts of THQ5 are formed. Satterfield and Yang have found, however, that the rate constants for the reactions of THQ5 → Q and DHQ → THQ1 are much smaller than those of the reactions THQ5 → DHQ and DHQ → hydrocarbons, respectively (*17*). Hence, THQ5 has mostly reacted back to DHQ and further to hydrocarbons before noticeable amounts of Q have been formed, while the formation of THQ1 cannot compete with the conversion of DHQ to hydrocarbons and THQ5.

In Fig. 2A–2B the DHQ conversions to hydrocarbons (N_{hc}) at 653 K and 623 K are plotted as a function of the position of the TMS in the Periodic System. The DHQ conversions to hydrocarbons (653 K) of the first-row TMS formed a U-shaped curve (Fig. 2A). V/C had the highest conversion, while the other first-row TMS catalyst had a conversion comparable to that of the carbon support. The DHQ conversions to hydrocarbons (N_{hc}) of the second-row TMS formed a volcano curve with a maximum at Rh/C at 653 K and 623 K (Fig. 2A–2B). At 623 K, Mo/C had a relatively high DHQ conversion to hydrocarbons compared to 653 K while the opposite was observed for the Pd/C catalyst. The DHQ conversion to hydrocarbons of the third-row TMS formed a volcano curve with a maximum at Ir/C, while W/C had the lowest N_{hc} at 653 K as well as at 623 K (Fig. 2A–2B).

The product distribution of the hydrocarbons is dependent on the DHQ conversion to hydrocarbons which in turn depends on the position of the TMS in the rows of the Periodic System (Table 1). The first-row TMS had a high selectivity for PBZ (n_{pbz} = 15–21%) and PCHE (n_{pche} = 26–36%) at 653 K. The unsaturated hydrocarbons were even formed to a higher extent in the DHQ–HDN than in the Q–HDN (*11, 21*).

As a result, the selectivity for PCH was relatively low and the N_{pch}/N_{pbz} ratio was lower than the ratios obtained in the Q–HDN experiments (*11, 21*) and also lower than the equilibrium ratio determined by Cochetto and Satterfield (*14*) for gas phase reactions (26 at 653 K, ≥100 at 623 K). The selectivities for the unsaturated hydrocarbons (n_{pbz} and n_{pche}) of the first-row TMS catalysts versus the position of the TMS in the Periodic Table form double maximum curves. This trend is similar to that for the HDS activities of these TMS catalysts (*4–6*) and this similarity is not surprising. Both reactions do not require preliminary hydrogenation reactions but involve only a ring-opening removal of the heteroatom and consecutive (de)hydrogenation reactions.

Not only the first-row TMS but also Mo/C and W/C had a high selectivity for PBZ and especially for PCHE at both temperatures. At 653 K their selectivity for PBZ was comparable to that of the first-row TMS, but that for PCHE was much higher. Almost 60% of the hydrocarbon products were thus unsaturated and the N_{pch}/N_{pbz} ratio was very low. In exactly the same way as the first-row TMS, the Mo/C and W/C catalysts had an even higher selectivity for PBZ and PCHE in the DHQ–HDN than in the Q–HDN (*11, 21*). The higher PCHE selectivity might be due to a selectivity higher for the reaction pathway via elimination of NH_3 from PCHA in the DHQ–HDN than that in the Q–HDN. However, the difference cannot be large since also the Q–HDN reaction (at least over Ni–Mo/Al_2O_3 catalysts) was reported to proceed for a major part via this reaction route and not via the OPA route. Some authors even claimed the same selectivities in both reactions (*14–18*). The high selectivity for PBZ is rather surprising as the reaction pathway via OPA is almost negligible in the DHQ–HDN due to the low OPA formation. It seems more likely that the high PCHE and PBZ selectivites are due to the high concentration of DHQ (N_{dhq}) in the DHQ–HDN reaction product mixture. DHQ has one of the highest adsorption coefficients (K = 2 kPa^{-1}) of all the compounds taking part in the DHQ–HDN network (DHQ ~ THQ5 > Q > THQ1 > OPA, probably K (PCHA) > K (DHQ), but PCHA reacts very fast) (*15–18, 23*) and the N_{dhq} was higher than in the Q–HDN (the equilibrium between the N-compounds was not established in the DHQ–HDN). A high coverage of the catalyst surface by DHQ will hinder the absorption of PCHE and PBZ and their secondary reactions to PCH. The ratio between the three hydrocarbons in the final reaction product is therefore only influenced to a minor extent by the secondary reactions of the hydrocarbons (*18, 21*). This means that PCHA was converted to a large extent to unsaturated hydrocarbons and that the equilibrium between PCH and PBZ cannot be reached as long as the presence of high percentages of N-compounds hinders the adsorption of PBZ and PCHE on the catalyst surface.

Some catalysts had a high PCH selectivity and a high N_{pch}/N_{pbz} ratio, which might be due to the direct formation of PCH by hydrogenolysis of the C–N bond of PCHA, i.e., without the (formation and) desorption of the PCHE intermediate from the catalyst surface. The PBZ and PCHE selectivities of the Re/C catalyst were considerably lower than in the Q–HDN (*11, 21*) and OPA–HDN (*21*) but the n_{pch}/n_{pbz} ratio was still relatively low at 653 K as well as at 623 K.

Cyclohexylamine HDN

Cyclohexylamine (CHA) was used as a substitute for the propylcyclohexylamine (PCHA) intermediate in the Q–HDN and DHQ–HDN reaction. Its denitrogenation (see Fig. 3 for abbreviations) proceeds via the cleavage of the C–N bond with the formation of CH (hydrogenolysis) or CHE (elimination). The CHA–HDN is a fast reaction and very high CHA–conversions to hydrocarbons (N_{hc}) were obtained at 653 K even with higher amounts of reactant and shorter reaction times. CH and BZ were the only hydrocarbon products at 653 K, while at temperatures below 593 K only CH and

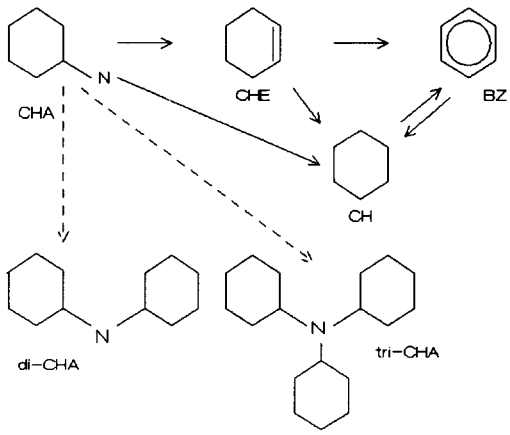

FIG. 3. Reaction network of the HDN of cyclohexylamine. CHA, cyclohexylamine; CHE, cyclohexene; di-CHA, dicyclohexylamine; CH, cyclohexane; BZ, benzene; tri-CHA, tricyclohexylamine.

CHE, and no BZ, were formed. This is in accordance with observations made by Schulz *et al.* in the HDN of aniline (*19*). Besides hydrocarbons and CHA the reaction product obtained at 653 K contained also significant amounts of dicyclohexylamine (di-CHA) and some tricyclohexylamine (tri-CHA). In Table 2 only the sum N_{by} of the byproducts has been reported. In accordance with results published by Geneste *et al.* for a Ni–W/Al_2O_3 catalyst (*24*), the formation of these byproducts was much higher at lower reaction temperatures (543–593 K) where it even exceeded the formation of hydrocarbons (Table 2). Dipropylcyclohexylamine and tripropylcyclohexylamine were not present in the reaction product mixture of the Q–HDN, DHQ–HDN, or OPA–HDN in considerable amounts, although traces of such compounds have been observed (*14–17*). The high amount of di-CHA and tri-CHA in the reaction product mixture of CHA–HDN must be due to the high amine concentration and low temperature used in CHA–HDN, since thermodynamically the formation of a dialkylamine from an amine and an olefin (or the disproportionation of two amine molecules to a dialkylamine and ammonia) is favored at high amine concentration and low temperature (*25, 26*). Furthermore, the formation of a di- or trialkylamine might be sterically hindered by the propyl-group of PCHA in the HDN of Q, DHQ, and OPA.

The side reaction of CHA to di- and tri-CHA constitutes a problem in the interpretation of the CHA–HDN results. If only the CH and CHE products are counted as denitrogenated products (N_{hc} in Table 2) then there are pronounced differences between the various TMS/C catalysts. If one considers, however, that most of the byproduct consist of di-CHA and that di-CHA can be considered to be a product which is already 50% denitrogenated (di-CHA = CHE + CHA, or di-CHA = 2 CHA + NH_3) one should add an amount equivalent to that of N_{by} to N_{hc} to obtain the true percent N-

TABLE 2

HDN of Cyclohexylamine
(4.8–5.5 MPa, 543–653 K, t = 3 h)

Catalyst[a]	Product composition[b]					
	N_{hc}	N_{ch}	N_{che}	N_{cha}	N_{by}	NR[c]
	T(sulf.) = 623 K, T(react.) = 593 K					
C	18	12	6	29	54	47
V/C	42	20	22	31	27	55
Cr/C	20	9	11	39	41	43
Mn/C	10	4	6	39	52	41
Fe/C	8	5	3	39	53	40
Co/C	27	7	19	37	36	45
Ni/C	34	9	25	35	31	50
	T(sulf.) = 623 K, T(react.) = 553 K					
Mo/C	23	8	15	31	46	47
Ru/C	38	22	16	25	37	55
Rh/C	29	25	4	30	41	50
Pd/C	12	9	3	43	45	39
	T(sulf.) = 623 K, T(react.) = 543 K					
W/C	2	1	2	47	50	36
Re/C	5	3	2	29	66	43
Os/C	15	12	3	25	60	47
Ir/C	16	14	2	32	51	44
Pt/C	4	1	4	29	66	43

[a] The metal loadings are as indicated in Table 1.
[b] N_x = cyclohexylamine conversion to product x. For details see Experimental section.
[c] NR = $(N_{hc} + N_{by})/(100 + N_{by})$.

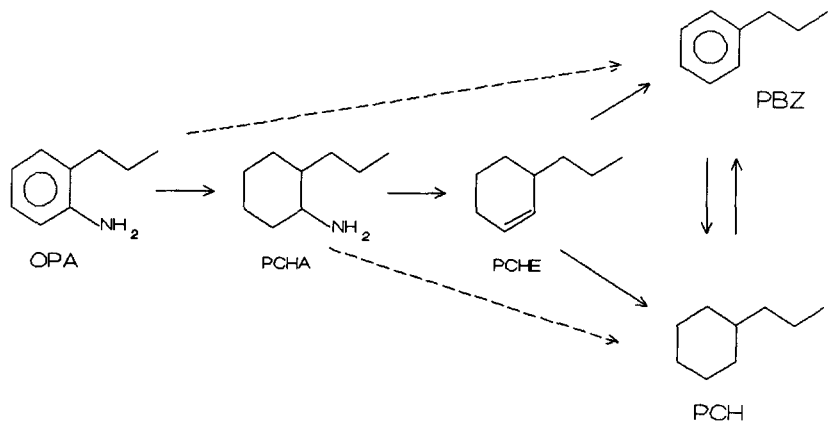

FIG. 4. Reaction network of the HDN of *o*-propylaniline. OPA, *o*-propylaniline; PCHA, propylcyclohexylamine; PCHE, propylcyclohexene; PBZ, propylbenzene; PCH, propylcyclohexane.

removal (NR in Table 2). In that case the differences between the various TMS/C catalysts of one particular row of the Periodic Table become small. The primary conclusion in that case in that the third-row TMS are somewhat more active than those of the second row, and that these in turn are more active than the first-row TMS (Table 2) (note the differences in reaction temperatures). Due to the high CHA-conversions to hydrocarbons (N_{hc}) no trends could be determined at 653 K. The CHA-conversions to hydrocarbons of the first row TMS at 593 K formed a shallow U-shaped curve with a minimum at Mn/C and Fe/C. There were volcano curves for the CHA conversion to hydrocarbons of the second- and third-row TMS at 553 K and 543 K, respectively. The Ru/C catalyst had the highest CHA–HDN conversion of the second-row TMS and the Os/C and Ir/C catalysts had the highest activities of the third-row TMS.

A comparison of the results presented in Tables 1 and 2 demonstrates that for all TMS/C catalysts the HDN of CHA is much faster than that of DHQ. This is in accordance with the fact that almost no PCHA was observed in the HDN of DHQ; once formed, PCHA reacts immediately to hydrocarbons. Why the primary amines CHA and PCHA are so much more reactive than the secondary amine DHQ is not clear, since usually a secondary amine is more basic than a primary amine and might be expected to have a higher adsorption coefficient. It may well be that while the elimination of NH_3 from PCHA occurs uninhibitedly, the ring-opening elimination of DHQ to PCHA is sterically somewhat hindered.

In contrast to the results of the Q- and DHQ–HDN (*11, 12, 21*) the CHA-conversions to hydrocarbons of the second- and third-row TMS differed only slightly. Such an observation has also been made for the activities of these TMS catalysts in the OPA–HDN (vide infra). It seems that there are no considerable differences between the activities of second- and third-row TMS catalysts in the HDN once the necessity of the ring-opening is eliminated. Trends comparable to those of the CHA-conversions to hydrocarbons were observed for some of the selectivities of the TMS catalysts in the CHA–HDN reactions (Table 2).

Orthopropylaniline HDN

The results of the OPA–HDN experiments are listed in Table 3 (see Fig. 4 for its HDN network and for abbreviations). OPA and traces of PCHA were the only N-con-

TABLE 3

HDN of *o*-Propylaniline

	T = 653 K				T = 613 K				T = 593 K			
	N_{hc}	n_{pch}	n_{pbz}	n_{pche}	N_{hc}	n_{pch}	n_{pbz}	n_{pche}	N_{hc}	n_{pch}	n_{pbz}	n_{pche}
C	7	49	27	24								
V(4.8)/C	21	66	22	12								
Cr(4.9)/C	19	67	21	12								
Mn(5.2)/C	12	43	29	28								
Fe(5.3)/C	13	48	30	22								
Co(5.6)/C	18	59	24	17								
Ni(5.6)/C	21	60	22	18								
Mo(8.8)/C	8	45	24	31	20	53	23	24				
Ru(9.2)/C	40	78	13	9	48	84	10	6				
Rh(9.3)/C	35	81	12	7	64	94	4	2				
Pd(9.6)/C	7	69	9	22	39	91	5	4				
W(15.5)/C	8	53	19	28	14	53	22	25	5	25	27	48
Re(15.7)/C	58	56	20	24	82	66	17	17	44	50	21	29
Os(16.0)/C	44	80	9	11	59	91	6	3	43	91	5	4
Ir(16.1)/C	65	91	7	2	82	94	5	1	42	93	5	2
Pt(16.3)/C	23	68	9	23	84	96	3	1	42	90	5	5

[a] The wt% of the metals are given within parentheses.

[b] Sulfidation as well as reaction was carried out at the indicated temperature. The reaction time was 1.5 h for the second- and third-row TMS at 653 K and 3 h in all other cases. N_{hc} is the mol% of OPA converted to hydrocarbons, $n_x = N_x/N_{hc}$ is the selectivity for compound x.

taining compounds found in the reaction product mixture. In contrast to the results obtained in the HDN of aniline over sulfided Ni–W/Al_2O_3 (*24*), no N-phenyl-cyclohexylamine-type products were observed. The amount of hydrocarbon byproducts was low (less than 2 mol%) and was not taken into account in the evaluation of the activity data, i.e., $N_{hc} + N_{opa} = 100$. The OPA-conversions to hydrocarbons are plotted as a function of the position of the TMS in the Periodic System in Figs. 5A (653 K) and 5B (613 and 593 K). Just as in the Q and DHQ–HDN test reactions, the periodic trends of the OPA conversions to hydrocarbons (653 K) of the first-row TMS formed a kind of U-shaped curve with a minimum at Mn/C and Fe/C, which is only slightly higher than that of the pure carbon support. The OPA conversions of the second-row TMS formed a volcano curve. As in the DHQ–HDN the shape of the curve and the position of the maximum were dependent on the reaction (and sulfidation) temperature. Mo/C and Pd/C had very low OPA conversions to hydrocarbons at 653 K while Ru/C had the highest OPA–HDN conversion (Fig. 5A). Although the high OPA conversion of Ru/C is different from the results of the Q- and DHQ–HDN experiments (*11, 12, 21*) in which Rh/C had the highest HDN conversion in the second row of TMS, it is not exceptional. Ru/C was also the best second-row TMS in the HDN of cyclohexylamine at 553 K and HDN of pyridine at 613 K (*13*), while unsupported Ru sulfide had the highest activity of the second-row TMS in the HDS of dibenzothiophene at 623 K (*4*). The maximum of the volcano curve for the OPA-conversions to hydrocarbons of the second-row TMS shifted to Rh/C at 613 K (Fig. 5B). Also the OPA-conversion to hydrocarbons of Pd/C became relatively higher at 613 K.

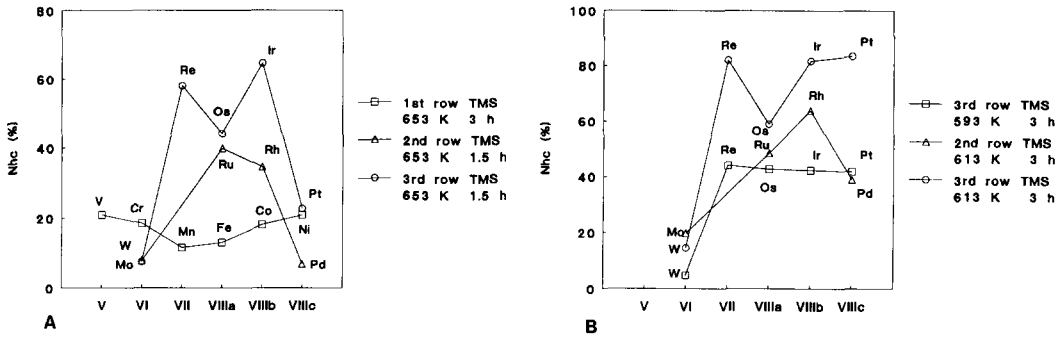

FIG. 5. Periodic trends for the *o*-propylaniline conversion to hydrocarbons (N_{hc}) over carbon-supported transition metal sulfide catalysts at 653 K (A), and 613 and 593 K (B).

The curve for the conversion of OPA to hydrocarbons of the third-row TMS was distorted and its shape changed with the reaction (and sulfidation) temperature (Figs. 5A–5B). At 653 K Re/C had almost as high a conversion as Ir/C, the best of all TMS catalysts (Fig. 5A). With this exception, the curve was similar to the volcano curve obtained in the Q–HDN and DHQ–HDN experiments (*11, 12, 21*). The shape of the curve was quite different at 613 K (Fig. 5B). Re/C, Ir/C and Pt/C had equal OPA–HDN conversions, while only Os/C and especially W/C had lower HDN conversions. Finally, at 593 K (Fig. 5B) Re/C, Os/C, Ir/C, and Pt/C had equal OPA–HDN conversions, and only W/C was less active. At all three reaction temperatures Re/C deviated from the usual volcano trend and had a very high OPA–HDN conversion.

A comparison of the OPA–HDN with the DHQ–HDN shows that at 653 K the conversion of DHQ to hydrocarbons is larger or equal to that of OPA for all TMS/C catalysts but Re/C. The HDN of DHQ at 623 K is, however, slower than the HDN of OPA at 613 K. Exceptions in this case are Mo/C and Ir/C, but the differences were small and it can safely be stated that all TMS/C catalysts would have had a higher conversion in the HDN of OPA if they had been measured at the same temperature, be it 623 or 613 K. The fact that the OPA to PCHA equilibrium is relatively more on the PCHA side at low temperature might be the reason for the crossover from a relatively faster HDN of OPA at the lower temperature to a faster HDN of DHQ at higher temperature.

The ring-opening (of DHQ or THQ1) or the preceding hydrogenation steps, rather than the subsequent N removal, is for most TMS/C catalysts the slowest step of the HDN of quinoline in the reaction route via DHQ as well as OPA under the given reaction conditions (*11, 12, 15, 19, 20*). As the ring-opening and the competitive, impeding adsorption of DHQ and other N-compounds are absent in the HDN of OPA, the conversion of OPA to hydrocarbons should be easier than the conversion of Q to hydrocarbons. At 653 K the conversion of OPA to hydrocarbons was indeed larger than the corresponding conversion of Q (*11, 21*) for all TMS/C catalysts. Thus, just as for the $NiMo/Al_2O_3$ catalysts (*15, 17*), the rate constants in the reactions from OPA to hydrocarbons are not limiting factors in the OPA route of the HDN of quinoline for any of our TMS/C catalysts.

Because n_{pch} is a monotonically increasing function of conversion (and n_{pbz} and n_{pche} are monotonically decreasing functions) (cf. Figs. 6C and 7C), the hydrocarbon selectivities of the TMS followed periodic trends similar to the conversions of OPA to hydrocarbons. Thus, the PCH selectivities $n_{pch} = 100 - n_{pbz} - n_{pche}$ of the first row TMS formed a U-shaped curve with a minimum

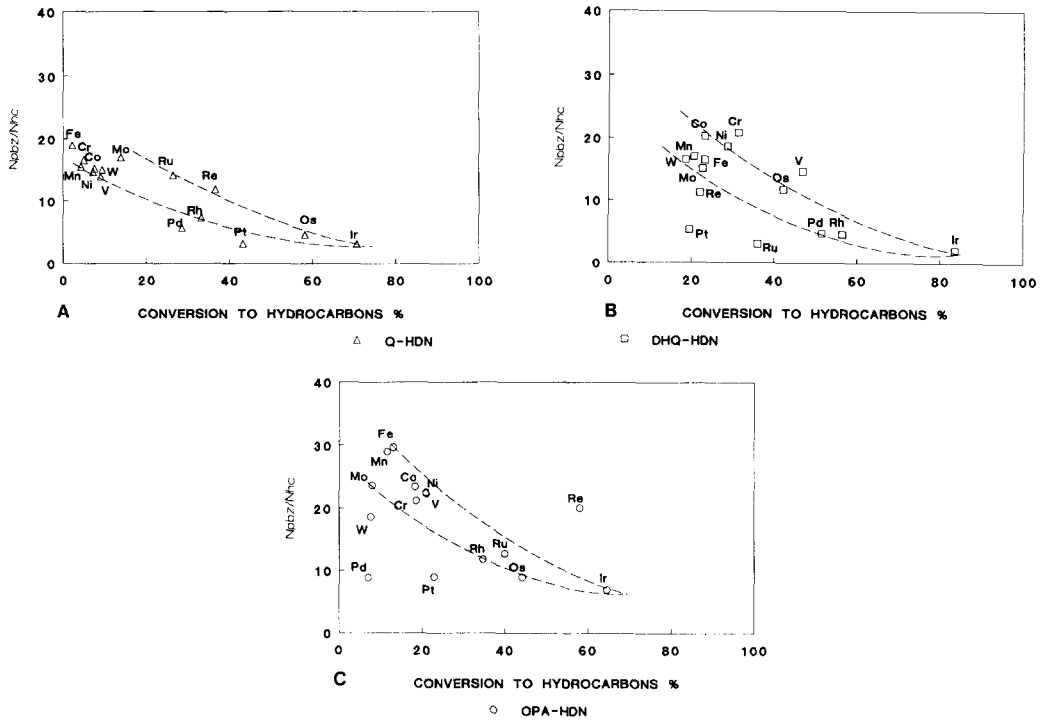

FIG. 6. Plots of the propylbenzene selectivity n_{pbz} versus the conversion to hydrocarbons N_{hc} over carbon-supported transition metal sulfide catalysts in the HDN of quinoline (A), decahydroquinoline (B), and *o*-propylaniline (C).

at Mn/C and Fe/C, while the propylbenzene and propylcyclohexene selectivities n_{pbz} and n_{pche} followed the reverse trend. The n_{pch} of the second row TMS formed a volcano curve with a maximum at Rh/C at 653 and 613 K, and the n_{pche} followed the reverse trend. The n_{pbz}, on the other hand, decreased continuously from group VI to VIII. The n_{pch} of the third-row TMS formed a volcano curve with maximum at Ir/C at 653 K, while the n_{pch} of Os/C, Ir/C, and Pt/C were the highest (>90%) and almost equal at 613 and 593 K. Again, the n_{pche} and n_{pbz} followed the reverse trend. The N_{pch}/N_{pbz} ratios were lower for TMS with low OPA conversions to hydrocarbons and in all cases but one they were lower than the thermodynamic equilibrium values (26 at 653 K and >100 at 613 and 593 K, all at p_{H2} = 4 MPa). Only Ir/C had at 653 K a N_{pch}/N_{pbz} ratio which was about equal to the equilibrium value.

The reaction of OPA to hydrocarbons forms part of the Q–HDN reaction network. A comparison of the OPA–HDN and Q–HDN conversions and product distributions might therefore give important indications about the reaction pathways of both reactions. Q–HDN proceeds for the major part via the DHQ and PCHA intermediates (cf. Fig. 1), while OPA–HDN is claimed to go via NH_3 removal from PCHA as well as via direct hydrogenolysis of OPA (*15, 17, 19, 20*). If OPA–HDN proceeds mainly via the PCHA intermediate, the product distribution of Q-, DHQ-, and OPA–HDN should be quite similar (*14, 15*). If on the other hand OPA–HDN proceeds to a high extent via hydrogenolysis of the aniline C–N bond with the direct formation of PBZ, the reaction product of OPA–HDN should contain more PBZ than the product of Q–HDN or DHQ–HDN. As Fig. 6 shows, the PBZ se-

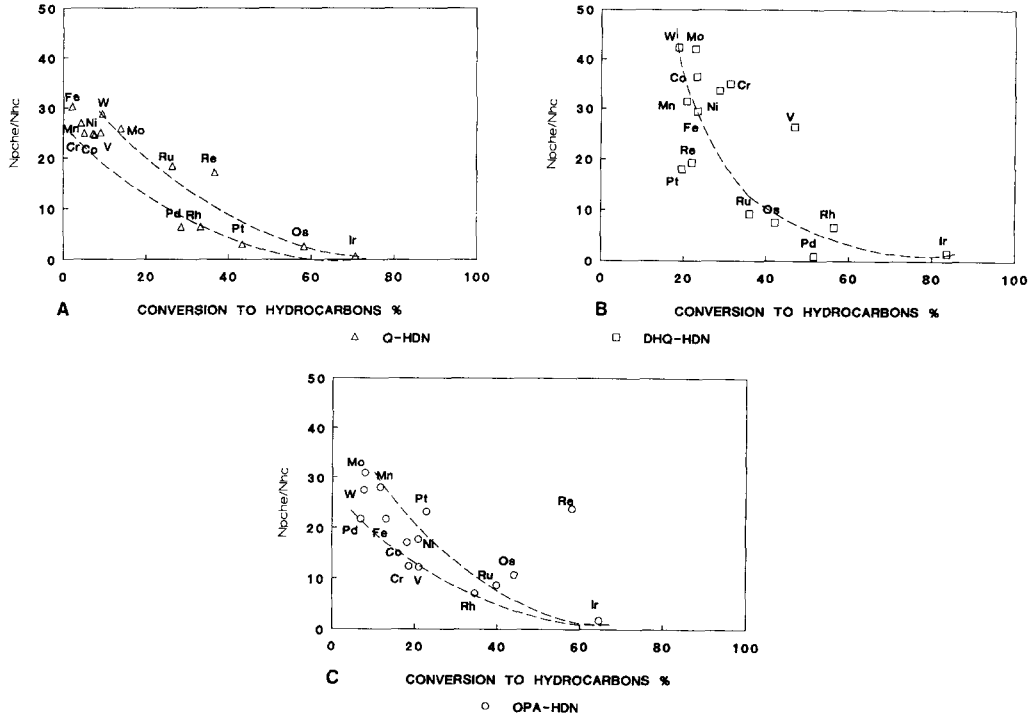

FIG. 7. Plots of the propylcyclohexene selectivity n_{pche} versus the conversion to hydrocarbons N_{hc} over carbon-supported transition metal sulfide catalysts in the HDN of quinoline (A), decahydroquinoline (B), and *o*-propylaniline (C).

lectivities of most TMS were indeed higher in the OPA–HDN than in the Q- or DHQ–HDN. On the other hand, the selectivity–conversion trends observed for most TMS in the OPA–HDN agree rather well with the trends observed in the study of the HDN of aniline over a $NiMo/Al_2O_3$ catalyst (*19*). In that study Schulz *et al.* proved by extrapolation of the cyclohexene selectivity to zero conversion that elimination is the almost exclusive reaction pathway in the HDN of aniline via cyclohexylamine, through cyclohexene to benzene and cyclohexane (*19*), and that it is not necessary to invoke the hydrogenolysis pathway of aniline to benzene. Apparently, even in the presence of aniline cyclohexene is able to adsorb on the catalyst surface and react to benzene and cyclohexane. The cyclohexane/benzene ratio is, however, determined by competing adsorption effects.

Most of the OPA results obtained with our TMS catalysts can be explained in exactly the same way as the aniline results for the $NiMo/Al_2O_3$ catalyst, suggesting that also in the HDN of OPA over these TMS catalysts the elimination pathway via PCHA is more important than the hydrogenolysis pathway. The N_{pche}/N_{pbz} and N_{pche}/N_{pch} ratios of all TMS catalysts were much larger than the thermodynamic equilibrium values determined for gas phase reactions (*14*), proving that the majority of PCHE must indeed have been formed prior to PBZ and PCH and thus via elimination of NH_3 from PCHA. The primary formation of PCHE also explains why the selectivity–conversion curve for PBZ lies higher in the HDN of OPA than in the HDN of Q (*11, 21*) and DHQ (Fig. 6), while the selectivity–conversion curve for PCHE is highest in the DHQ–HDN (Fig. 7). In Q–HDN as well as

in DHQ–HDN, the n_{pbz} are smaller than the n_{pche} for most TMS/C catalysts, while the reverse is true for OPA–HDN. The reason could be the stronger adsorption of DHQ than of OPA, making the reaction of PCHE to PBZ less hindered by competitive adsorption in the OPA–HDN. Although the conversions of PCHE into PCH and PBZ have been indicated by separate arrows in Figs. 1 and 4, we have at present no evidence to exclude the disproportionation reaction 3 PCHE → 2 PCH + PBZ as the source of PCH and PBZ.

Not all TMS/C catalysts followed the above selectivity–conversion relationship. Re/C and to some extent also Pd/C and Pt/C formed clear exceptions. Re/C had much higher PBZ and PCHE selectivities (and consequently a much lower PCH selectivity) than was to be expected from its high conversion of OPA to hydrocarbons and the general selectivity trends observed for the majority of the TMS/C catalysts (Figs. 6C and 7C). Similar deviating selectivities were observed for Re/C in the Q–HDN (*11*, *21*) (Figs. 6A and 7A). The high activity for the denitrogenation of OPA combined with the high selectivity for unsaturated hydrocarbons make Re/C an exception among the TMS/C catalysts. It might be that for this catalyst the hydrogenolysis pathway from OPA to PBZ plays a more important role than for the other catalysts. On the other hand, the PCHE yield for Re/C was larger than the PBZ yield at all three reaction temperatures and the N_{pche}/N_{pbz} and N_{pche}/N_{pch} rations were much larger than the thermodynamic equilibrium ratios. This proves that the elimination pathway OPA–PCHA–PCHE also plays an important role for Re/C. Further studies must be awaited before a definite conclusion can be made about the relative contributions of both pathways for Re/C. The selectivities of Pd/C and Pt/C for propylbenzene were lower and those for propylcyclohexane higher than expected from their conversions of OPA to hydrocarbons (Fig. 6A). These selectivities seem to be more in line with the hydrogenation activities of the Pd and Pt metals. In this context it should be noted that we have no information about the actual composition of the catalysts during the catalytic reaction and that Pecoraro and Chianelli have indicated that quite a few of the group VIII metal sulfides might decompose into metal and sulfur under reaction conditions (*4*).

CONCLUSIONS

The OPA conversion to hydrocarbons of the carbon-supported first-row transition metal sulfide catalysts formed a U-shaped curve with a minimum at Mn and Fe. The OPA conversions to hydrocarbons of the second-row TMS formed a volcano curve with a maximum at Ru/C (653 K) or Rh/C (613 K). The OPA conversions to hydrocarbons of the third-row TMS formed a kind of volcano curve with a maximum at Ir/C but this curve was distorted. Some of the third-row TMS and especially Re/C had almost as high a conversion to hydrocarbons as Ir/C at 593 and 613 K. The changes of the trends with temperature were due to the differences in the surface composition of the catalysts and in the reaction mechanism of the OPA–HDN at different pretreatment and reaction conditions. All the TMS catalysts tested in the OPA–HDN had a high selectivity for propylbenzene, but the selectivity of the Re/C catalyst was exceptionally high.

The decahydroquinoline and cyclohexylamine conversions to hydrocarbons of the carbon-supported first-row transition metal sulfide catalysts formed U-shaped curves with a minimum around Mn/C and Fe/C. The conversions of the second- and third-row transition metal sulfide catalysts formed volcano curves with maxima at Rh/C and Ir/C, respectively. The trends for the HDN activities and selectivities depended on the sulfidation procedure as well as on the actual reaction conditions (temperature, reactant). The consecutive conversions of hydrocarbons on the catalyst surface were inhibited in the presence of stronger adsorbing N-compounds and the TMS catalysts had a relatively high selectivity for propylbenzene

and especially propylcyclohexene in the HDN of quinoline. The high selectivity for propylbenzene indicates that even the fully saturated propylcyclohexylamine intermediate can be converted to aromatic products.

ACKNOWLEDGMENTS

This investigation was supported by the Netherlands Foundation for Chemical Research (SON) with financial aid from the Netherlands Technology Foundation (STW).

REFERENCES

1. Sinfelt, J. H., *Prog. Solid State Chem.* **10,** 55 (1975).
2. Ledoux, M. J., *J. Catal.* **70,** 375 (1981).
3. Fung, S. C., and Sinfelt, J. H., *J. Catal.* **103,** 220 (1987).
4. Pecoraro, T. A., and Chianelli, R. R., *J. Catal.* **67,** 430 (1981).
5. Vissers, J. P. R., Groot, C. K., van Oers, E. M., de Beer, V. H. J., and Prins, R., *Bull. Soc. Chim. Belg.* **93,** 813 (1984).
6. Ledoux, M. J., Michaux, O., Agostini, G., and Pannisod, P., *J. Catal.* **102,** 275 (1986).
7. Harris, S., and Chianelli, R. R., *J. Catal.* **86,** 400 (1984).
8. Harris, S., and Chianelli, R. R., *Chem. Phys. Lett.* **101,** 603 (1983).
9. Harris, S., *Chem. Phys.* **67,** 229 (1982).
10. Chianelli, R. R., Pecoraro, T. A., Halbert, T. R., Pan, V. H., and Stiefel, E. I., *J. Catal.* **86,** 226 (1984).
11. Eijsbouts, S., de Beer, V. H. J., and Prins, R., *J. Catal.* **109,** 217 (1988).
12. Sudhakar, C., Eijsbouts, S., de Beer, V. H. J., and Prins, R., *Bull. Soc. Chim. Belg.* **96,** 885 (1987).
13. Ledoux, M., and Djellouli, B., *J. Catal.* **115,** 580 (1989).
14. Cochetto, J. F., and Satterfield, C. N., *Ind. Eng. Chem. Process Des. Dev.* **20,** 49 (1981).
15. Satterfield, C. N., and Cochetto, J. F., *Ind. Eng. Chem. Process Des. Dev.* **20,** 53 (1981).
16. Satterfield, C. N., and Gültekin, S., *Ind. Eng. Chem. Process Des. Dev.* **20,** 62 (1981).
17. Satterfield, C. N., and Yang, S. H., *Ind. Eng. Chem. Process Des. Dev.* **23,** 11 (1984).
18. Satterfield, C. N., and Smith, C. M., *Ind. Eng. Chem. Process Des. Dev.* **25,** 942 (1986).
19. Schulz, H., Schon, M., and Rahman, N. M., *Stud. Surf. Sci. Catal.* **27,** 201 (1986).
20. Gioia, F., and Lee, V., *Ind. Eng. Chem. Process Des. Dev.* **25,** 918 (1986).
21. Eijsbouts, S., de Beer, V. H. J., and Prins, R., *J. Catal.* **127,** 618 (1991).
22. Tajik, S., *Ind. Eng. Chem. Res.*, in press.
23. La Vopa, V., and Satterfield, C. N., *J. Catal.* **110,** 375 (1988).
24. Geneste, P., Moulinas, C., and Olivé, J. L., *J. Catal.* **105,** 254 (1987).
25. Sonnemans, J., and Mars, P., *J. Catal.* **34,** 215 (1974).
26. Sonnemans, J., Neijens, W. J., and Mars, P., *J. Catal.* **34,** 230 (1974).